

SUPPORTING INFORMATION TO:

Role of hydrophobic interactions in the encounter complex formation of plastocyanin and cytochrome *f* complex revealed by paramagnetic NMR spectroscopy

Sandra Scanu, Johannes Förster, G. Matthias Ullmann and Marcellus Ubbink

Details on mutagenesis

Table S1 gives the sequences of the primers used for mutagenesis. In each primer a silent mutation (bold) was designed to remove or to introduce an extra restriction site. In the cases of Q7C and Q38C mutations, the codon-changing mutations (bold, underlined) introduced at the same time a restriction site for the enzyme *Apa*LI and removed a restriction site for *Mn*II, respectively. For A63C and A125C mutations, restriction sites for the enzymes *Bst*XI and *Xma*I, respectively, were introduced at the 5' end of the forward primers. In the primers for the S181C mutation, the restriction site for the enzyme *Mn*II was inserted at the 3' end of the forward primer. In the case of the Q242C mutant, the restriction site for the enzyme *Taq*I was introduced next to the codon for the cysteine mutation. The presence of the mutations was verified by DNA sequencing.

Table S1. Nucleotide sequence of the primers used in site-directed mutagenesis of Cyt *f*. Codon-changing mutations are shown in bold, italic and underlined; silent mutations are in bold.

Mutation	Primer sequence
Q7C	FWD: 5'-gcatatcctttctggg'gcag <u>ggc</u> acttaccag-3'
Q38C	FWD: 5'-gccacagaagtgaagttcct <u>ggc</u> tcctactaccgacaccg-3'
A63C	FWD: 5'-ccagcgtccaacaagttggt <u>ggc</u> gatggctctaagg-3'
Q125C	FWD: 5'-cccggggaacagtat <u>ggc</u> gaaatcgtcttcctgttcttctcccaacccc-3'
S181C	FWD: 5'-gcgctgctgctaccggtacaatt <u>ggc</u> aagattgctaacaagagggcg-3'
Q242C	FWD: 5'-ccctaacgttggtggttcggt <u>ggc</u> ctcgacgcagaaattgtctcc-3'

Calculation of PCS

The average intermolecular PCS from the ferric heme iron of Cyt *f* to the backbone amide atoms in all Pc conformers was calculated and compared with the experimental PCS previously measured in the wild type complex.^{S1} The equation used for the PCS calculation, assuming an axial magnetic susceptibility tensor oriented along the Fe-Y1 vector,^{S2} was:

$$\Delta\delta_{PCS} = \frac{\Delta\chi_{ax}}{12\pi r^3} (3 \cos^2 \theta - 1) \quad (\text{Equation S1})$$

In which $\Delta\delta_{PCS}$ is the size of the PCS, r is the distance between heme iron and observed Pc nucleus, and θ is the angle between Pc nucleus, heme iron and the nitrogen of the amine group of Y1 in Cyt *f*. $\Delta\chi_{ax}$ is the size of the axial magnetic component of the susceptibility tensor, derived from the g -tensor values measured by EPR spectroscopy on plant Cyt *f* and taken to be $7 \times 10^{-32} \text{ m}^3$, as previously reported for *Nostoc* Cyt *f*.^{S1} To correct for the possible difference in tensor size for the temperatures of EPR and NMR measurements, 10 K and 298 K, respectively, the $\Delta\chi_{ax}$ was varied from 0.7 to $8.4 \times 10^{-32} \text{ m}^3$.

The agreement between observed (PCS^{obs}) and calculated (PCS^{calc}) PCS was expressed by the PCS Q factor, defined as:

$$Q_{PCS} = \frac{\sqrt{\sum (PCS^{obs} - PCS^{calc})^2}}{\sqrt{\sum (|PCS^{obs}| + |PCS^{calc}|)^2}} \quad (\text{Equation S2})$$

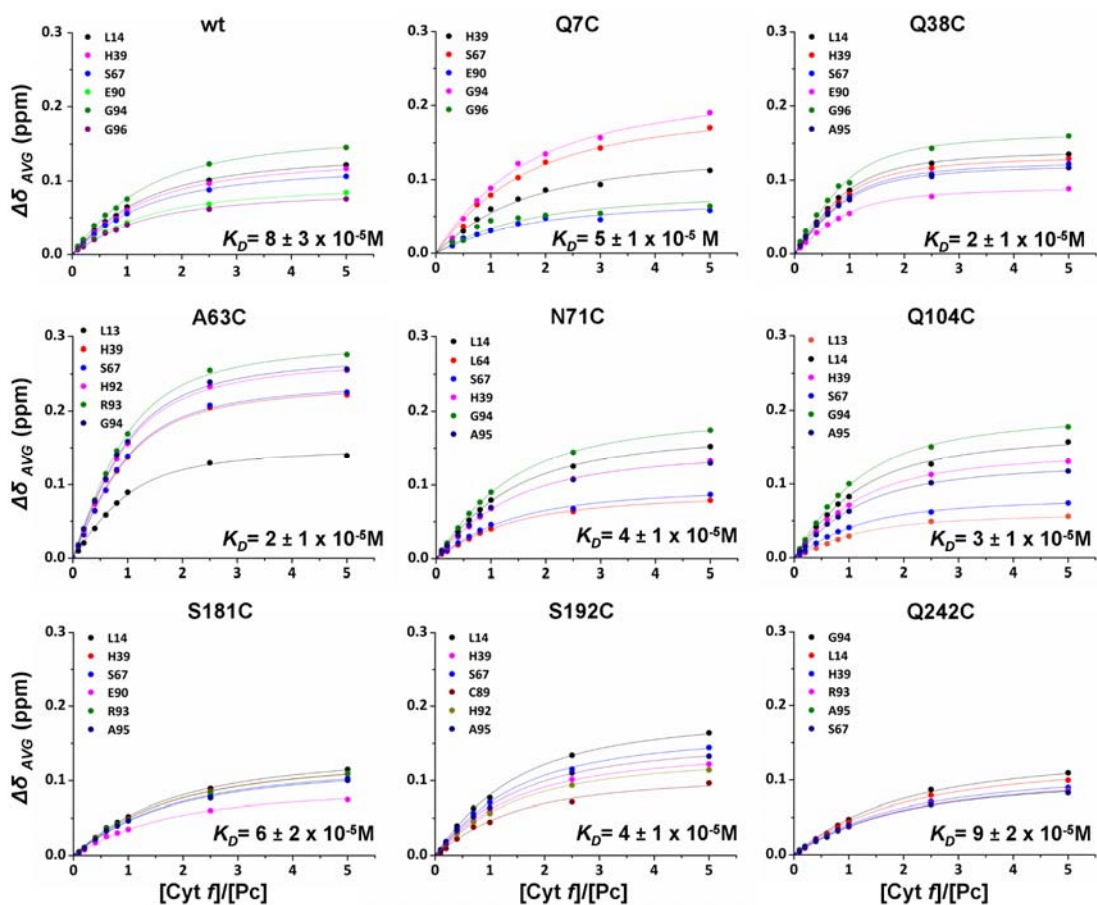


Figure S1. The interaction of *Nostoc* Zn-substituted Pc with wild-type Cyt *f* and MTS-conjugated variants. The binding curves for selected residues were fitted globally to a 1:1 binding model.

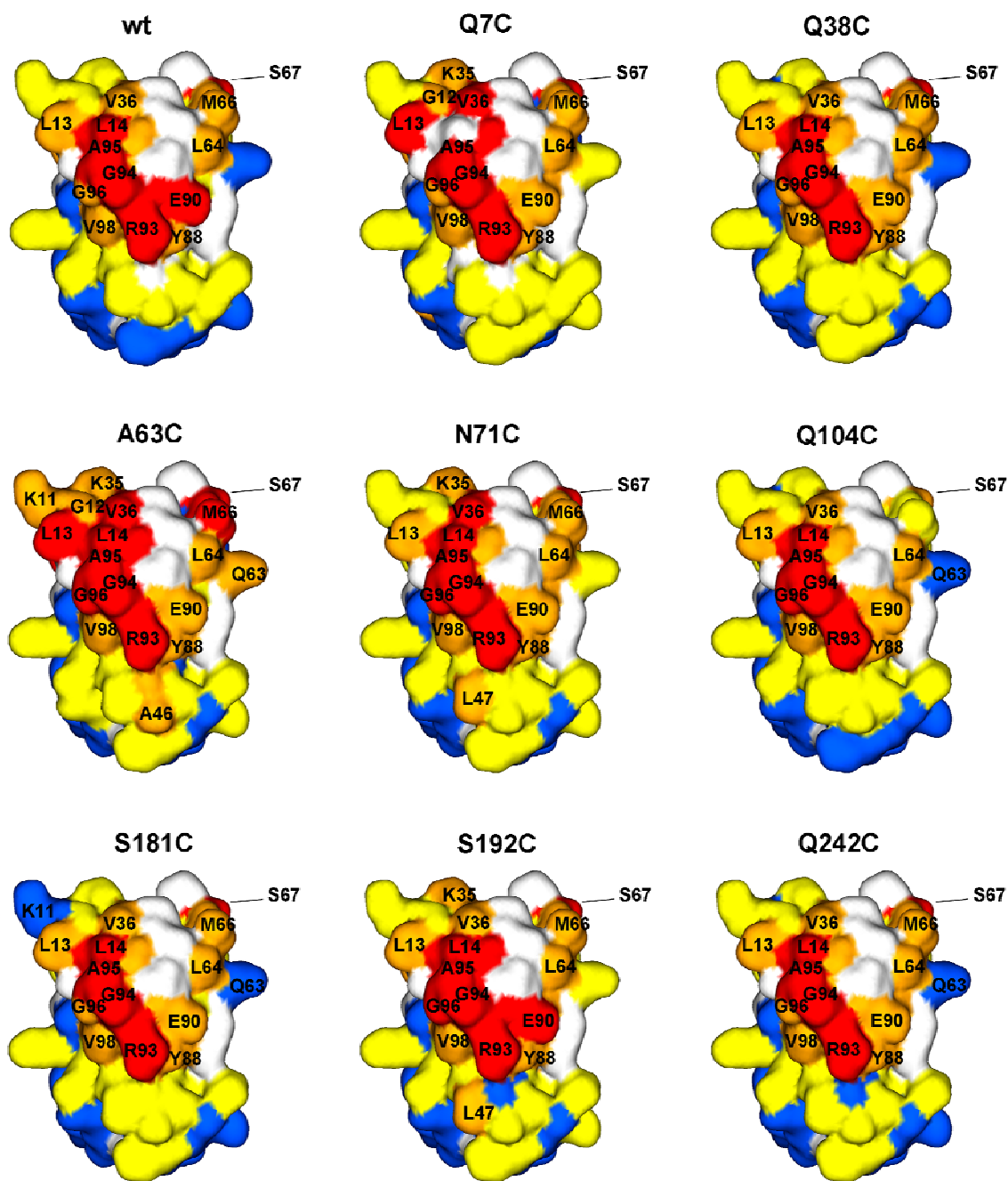


Figure S2. Chemical shift perturbation maps of *Nostoc* Zn-substituted Pc in the presence of wild-type and MTS-conjugated Cyt *f*, colour-coded on a surface model of Pc (PDB entry 2GIM), with red, $\Delta\delta_{avg} \geq 0.10$ ppm; orange, $\Delta\delta_{avg} \geq 0.05$ ppm; yellow, $\Delta\delta_{avg} \geq 0.02$ ppm; blue, $\Delta\delta_{avg} < 0.02$ ppm. Prolines and residues with overlapping resonances are in white.

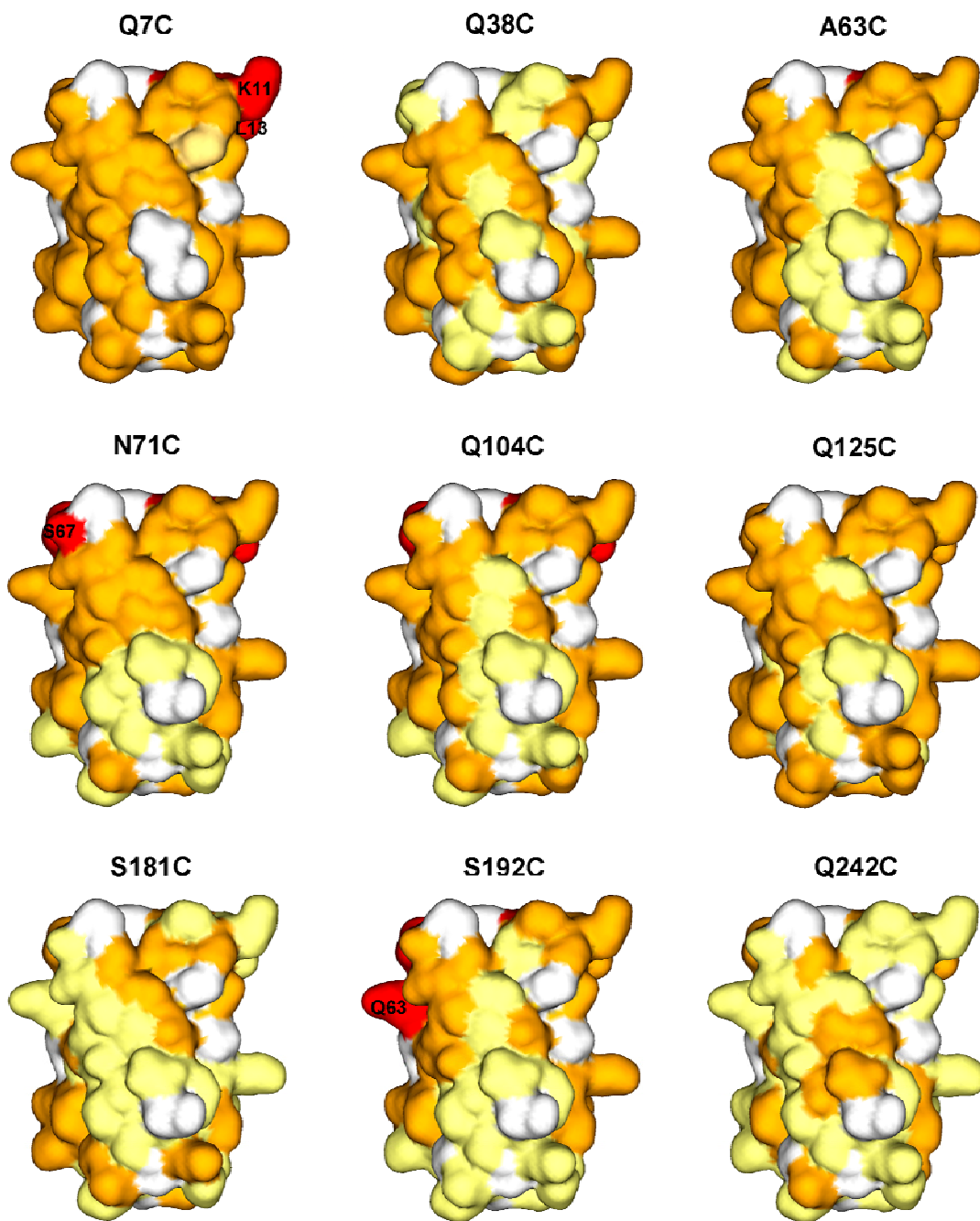


Figure S3. PRE maps of Zn-substituted Pc bound to MTSL-conjugated Cyt *f*, color-coded on a surface model of Pc (PDB entry 2GIM), the sites of spin label attachment are indicated in Figure 1, central panel. Red, $\Gamma_2 \geq 200 \text{ s}^{-1}$; orange, $10 \text{ s}^{-1} < \Gamma_2 < 200 \text{ s}^{-1}$ and yellow $\Gamma_2 \leq 10 \text{ s}^{-1}$. Prolines and residues with overlapping resonances are white.

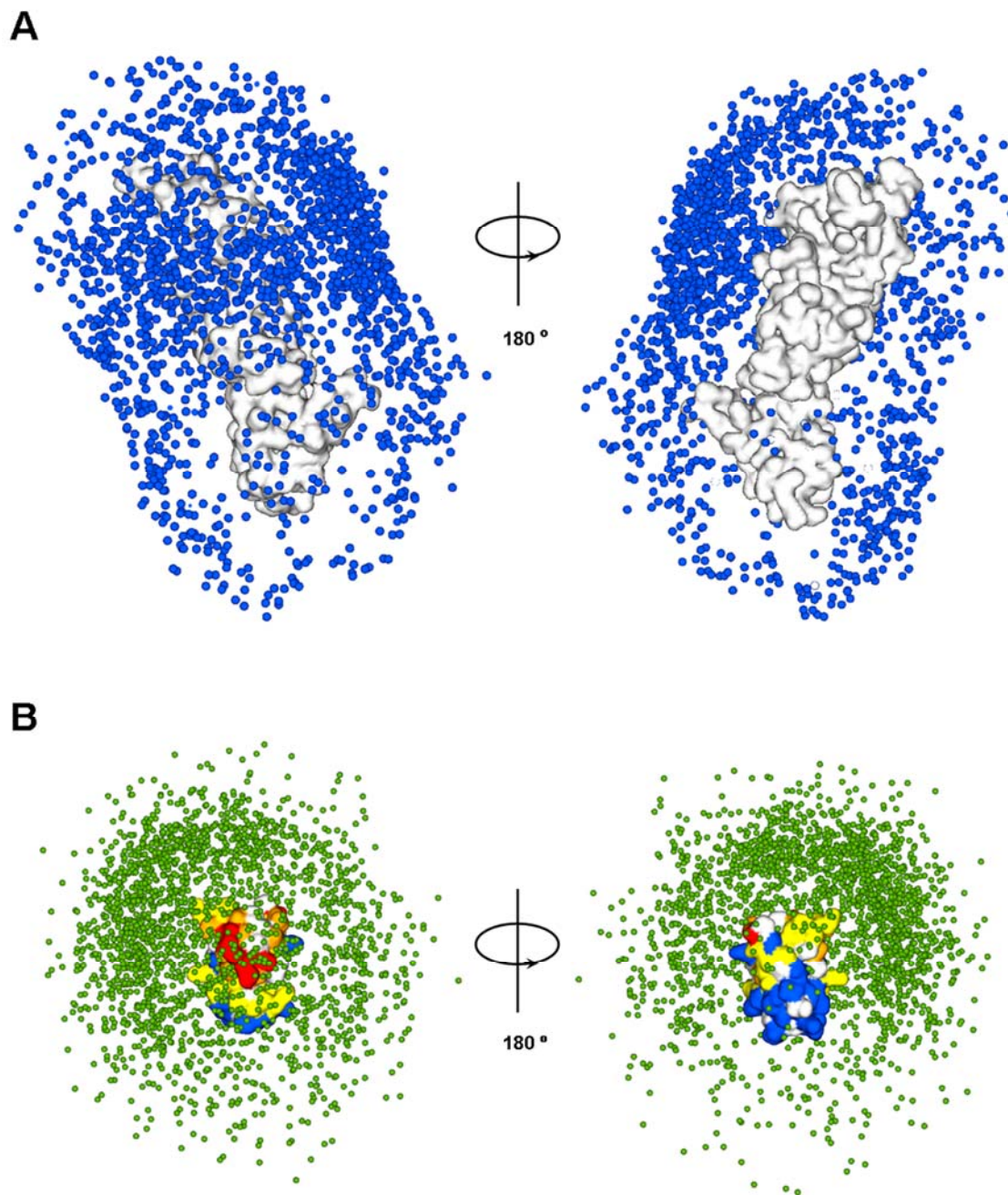


Figure S4. Encounter complex of the *Nostoc* Pc-Cyt *f* complex obtained by random selection of 2000 structures from the MC simulations. A) Cyt *f* is shown as a white surface and Pc centers-of-mass are represented by blue spheres. B) Pc is shown as a surface color-coded according to the CSP in the presence of wild-type Cyt *f* and Cyt *f* centers-of-mass are represented by green spheres.

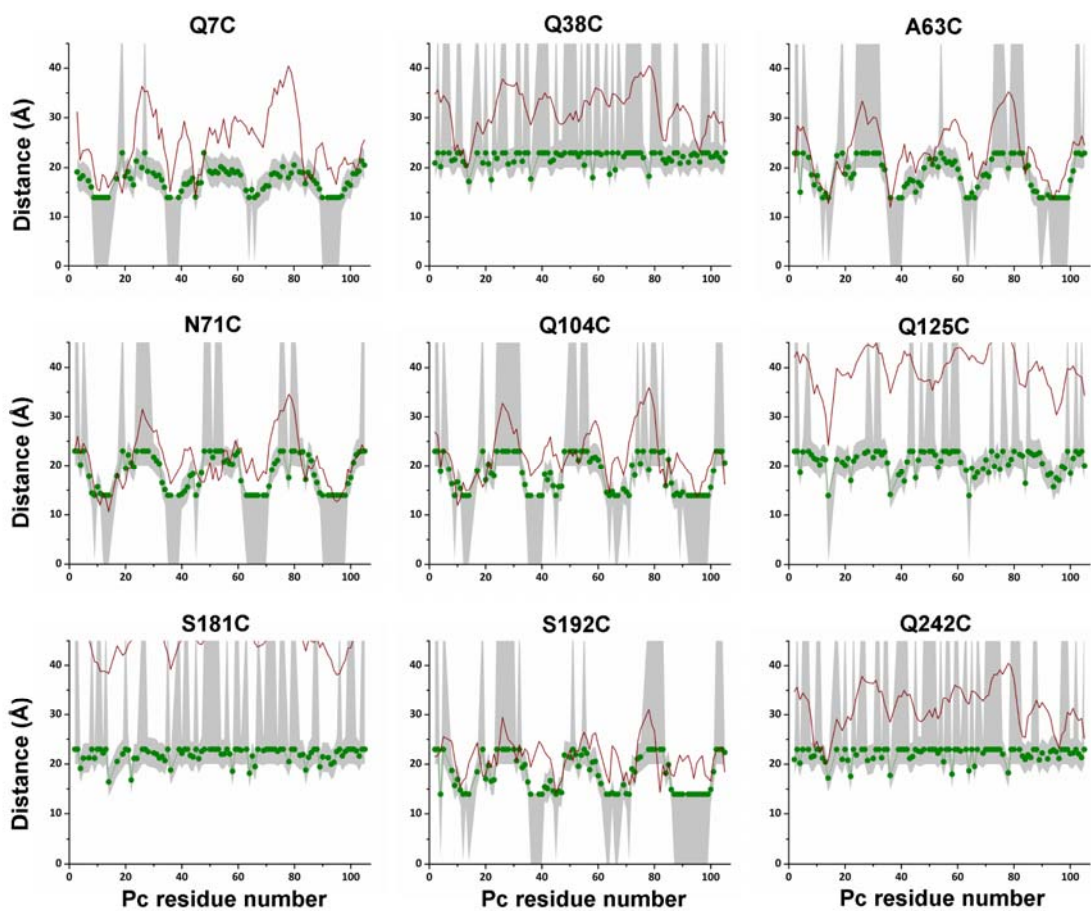


Figure S5. Comparison between back-calculated averaged distances from 2000 randomly selected structures of the MC simulation (red line) assuming $f_l=1$ and the experimental distances (green circles and lines). The grey areas indicate the error margins of experimental data.

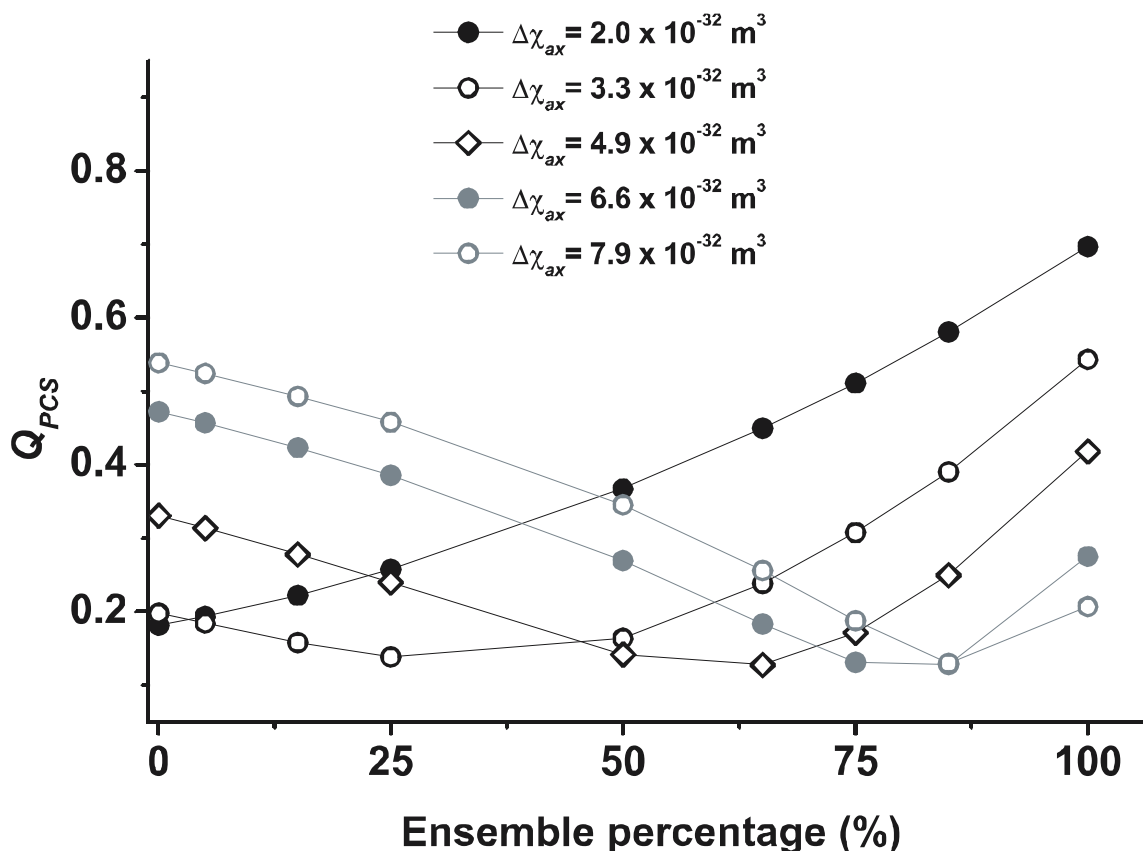


Figure S6. Q factors calculated for a combination of experimental PCS measured for the specific complex and back-calculated PCS from the encounter complex obtained at different fraction population of the encounter complex (f_i). The Q factors were calculated for different values of a scaling factor for the size of the axial component of the magnetic susceptibility tensor.

Reference List

- S1. Diaz-Moreno, I.; Diaz-Quintana, A.; De la Rosa, M. A.; Ubbink, M. *J. Biol. Chem.* **2005**, *280*, 35784.
- S2. Ubbink, M.; Ejdeback, M.; Karlsson, B. G.; Bendall, D. S. *Structure* **1998**, *6*, 323-335.